Simulation and performance optimization of GaAs/GaSb tandem solar cell

Fatima Zahra Kharchich[1,*], and *Abdellatif* Khamlichi[1]

[1]Laboratory SCD, ENSA Tetouan, University Abdelmalek Essaadi, 93002 Tetouan, Morocco

Abstract. Multi-junction solar cells provide the highest efficiencies. Intense research activity is being held with the aim to increase the actual performance reached by these cells. Harvesting most of the solar spectrum and finding the optimum design variables in terms of structural parameters and carrier concentrations are the main topics being investigated by solar developers. The GaAs/GaSb based dual-junction solar cell was found suitable for the best absorption of solar spectrum. In this work, an optimization approach was applied to fix the optimal parameters of the top base layer of this structure that provide the maximum efficiency. To achieve this, a series of numerical simulations were carried out by means of Silvaco ATLAS software under standard AM1.5G spectrum where thicknesses and doping levels of the top base layer were varied. The obtained optimal structure yields a power conversion efficiency of 41.65% with open circuit voltage of $1.78\,V$, short circuit current of $35.72\,mA/cm^2$ and fill factor of 90.16%. The performance of the GaAs/GaSb dual-junction solar cell was further improved by using sunlight concentration. A conversion power efficiency of 45.78% at 60sun light concentration was attained. It was found also that above this level of concentration ratio the detriment effect of shunt resistance dominates.

1 Introduction

Owing to their attractive electrical and optical properties, the III-V semi-conducting materials have received huge consideration from the community of solar cells developers. These materials show a strong resistance against irradiation, a high absorption coefficient as well as the ability to tune their band gap (from 0.3 to $2.3eV$) through elemental compositions change [1-2]. A wider range of the solar spectrum can then be covered. Semiconductor alloys have then found a wide use in solar cells fabrication. It was established that multi-junction devices offer enhanced performance due to a ramification effect affecting energy conversion, which becomes more effective than with the conventional silicon based cells [3].

The basic idea sustaining multi-junction solar cells is stacking multiple p-n junctions one on top of each other to enable broadening of the absorbed solar spectrum [4]. Each sub-cell is designed to respond in a specific part of the solar spectrum. This concept was found to be the only one that was successfully commercialized among the other ways of high efficiency designs [5-6].

Multi-junction solar cells having dual or triple junctions made of InGaP/GaAs and InGaP/GaAs/Ge materials are among the most studied configurations. These combinations have shown an excellent bandgap arrangement in lattice-matched systems [7]. However, they only use the solar spectrum up to a wavelength of $900\,nm$ [8]. Whereas, the GaSb based multi-junction solar cells, like GaAs/GaSb and InGaP/GaAs/GaSb, can utilize much larger spectral region which extends to the infrared part (up to $1800nm$) [9].

The first dual-junction solar cells were made in 1985 [10]. Since then, extensive studies have been undertaken to improve the power conversion efficiency. InGaP/GaAs dual-junction solar cells grown using D-HVPE have reached an efficiency of 24.9% [11-12]. Later, tandem cells made of InGaP/GaAs and fabricated using the triple-chamber HVPE system have attained a record efficiency of 28.3% [13]. Recently, the InGaP/GaAs/Ge triple-junction was reported with an efficiency of 29.78% [14], while GaAs/GaSb tandem cell has shown conversion efficiency up to 32.6% at 100sun under AM1.5D [15].

The InGaP/GaSb based dual-junction solar cell has shown the successful integration of antimonide into the multi-junction solar cells. It enabled reaching an efficiency of 44.05% under 1000suns for the AM1.5G spectrum [16]. The dual-junction architecture was found to be more attractive than the more complex and expensive triple and quadruple junctions based structures [17-18]. A theoretical study has already announced an efficiency of 50% for the GaAs/GaSb dual-junction at 1000sun [19].

The theoretical simulations have shown that higher efficiencies are quite possible. The complex structure of the multi-junction devices and the specific interactions existing between their different layers make in fact their experimental optimization a hard and expensive task.

* Corresponding author: kharchichfatima@gmail.com

© The Authors, published by EDP Sciences. This is an open access article distributed under the terms of the Creative Commons Attribution License 4.0 (http://creativecommons.org/licenses/by/4.0/).

The process of building an experimental prototype to be just tested once results to be effort and time consuming. Hence, developers rely more on simulation tools to perform parametric based studies towards achieving the best possible design. Experimentation is conducted at the final stage to validate the findings.

In the present work, a new GaAs/GaSb dual-junction solar cell is investigated numerically by using Silvaco ATLAS Software. Optimization of the design of the proposed structure is achieved through a parametric study including the following variables: top base layer thickness and carrier concentration. Then, the electrical performance of the cell will be analyzed at different sunlight illumination in the range of 1sun and 120sun.

2 Simulation of solar cells under Silvaco ATLAS software

2.1 Architecture of the studied solar cell

The studied solar cell is made of a GaAs top cell connected through a InGaP/InGaP tunnel junction to a GaSb bottom cell. Fig. A depicts the structure of the considered dual-junction solar cell. This figure indicates thickness, type and concentration of doping for each layer. Selection of this particular architecture is based on previous studies presented in [19-20].

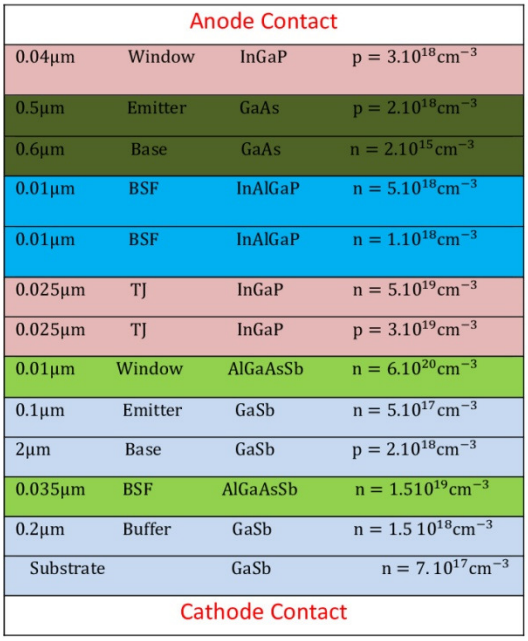

Fig.1. Schematic diagram of the studied GaAs/GaSb dual-junction solar cell structure.

The numerical simulation is carried out under AM1.5 illumination and 300*K*. Silvaco ATLAS software is used for this purpose. ATLAS is a physically-based solar simulator that uses the Finite Element Method. It provides a reliable insight into the physical phenomena involved throughout the cell structure operation [21-22]. The software can predict the electrical behaviour of semiconductor devices by solving a set of differential equations coupling electrostatic field and carrier densities [23]. For the most accurate modelling, ATLAS offers a wide variety of physics based model which include: CONMOB (concentration dependent mobility), SRH (Shockley-Read-Hall), OPTR (OPTtical Recombination model) and Auger. In the present simulations use is made of CONMOB, OPTR, Auger, SRH, bandgap narrowing (BGN) and Fermi Dirac statistics models.

Table 1 gives the parameters used in simulations performed in this work. They were taken from existing literature [20,23].

Table 1. Physical parameters values used in this work.

Material	InGaP	GaAs	GaSb
Band gap	1.90	1.42	0.72
Electron mobility	1945	8800	15
Hole mobility	141	400	15
Permittivity	11.6	13.1	15.7

2.2 Main characteristics of solar cells

Performance evaluation of a solar cell is habitually conducted by examining its main electrical characteristics. These constitute the first concern to consider during the optimization process of a given architecture. The electrical characteristics include the open-circuit voltage $V_{OC}(V)$, the short-circuit current density $J_{sc}(mA/cm^2)$, the conversion efficiency $\eta(\%)$ and the fill factor $FF(\%)$. They are defined as follows [24-25]:

$$J_{sc} = \int_{\lambda_1}^{\lambda_2} E.SR(\lambda)\, d\lambda \tag{1}$$

$$V_{OC} = \frac{bk_B T_C}{q} \ln\left(\frac{J_{sc}}{J_0} + 1\right) \tag{2}$$

$$FF = \frac{P_{\max}}{J_{sc} V_{OC}} \tag{3}$$

$$\eta = \frac{J_{sc} V_{OC} FF}{P_{in}} \tag{4}$$

where $SR(\lambda)$ is the spectrum response, λ the wavelength (nm), E the solar irradiance (W/m^2), J_0 the dark current density (A), k_B the Boltzmann constant, n the diode ideality factor, T_C cell temperature (K), q the unit charge $(1eV)$, $P_{\max}$ the

maximum power (W) and P_{in} is the incident power (W).

3 Results and discussion

3.1 Influence of top base layer parameters on solar cell performance

3.1.1 Effect of base thickness

Typically, the base in a solar cell is generally the thickest and the least doped layer among all the sub-cell layers. This essential pat of a multi-junction solar cell is to be carefully designed as it monitors to a high degree the whole performance characteristics of the device. To assess the effect of the base layer parameters on the electrical characteristics, the response of the solar cell was simulated for different base thicknesses while keeping constant the other parameters of the structure.

Fig. 2 gives the obtained voltage V_{OC} versus the base layer thickness in μm. Fig. 3 gives the fill factor FF versus the base layer thickness. Fig. 4 gives the current density J_{sc} versus the base layer thickness. Fig.5 gives the efficiency versus the base layer thickness.

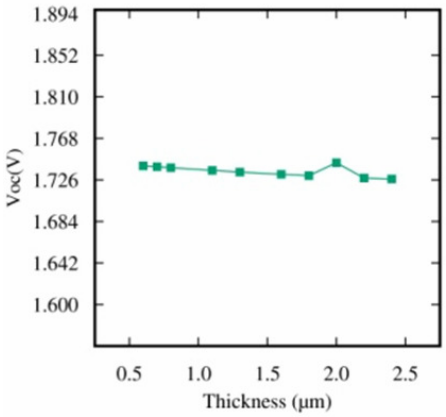

Fig. 2. Variation of solar cell open-circuit voltage versus the base thickness.

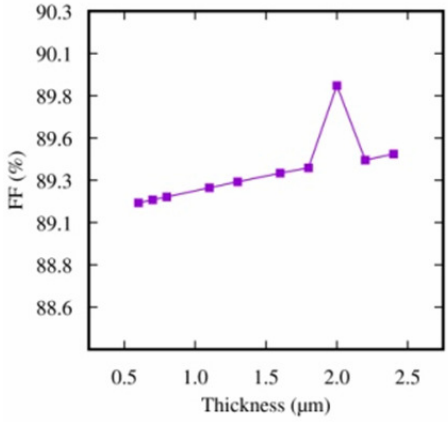

Fig. 3. Variation of solar cell fill factor versus the base layer thickness.

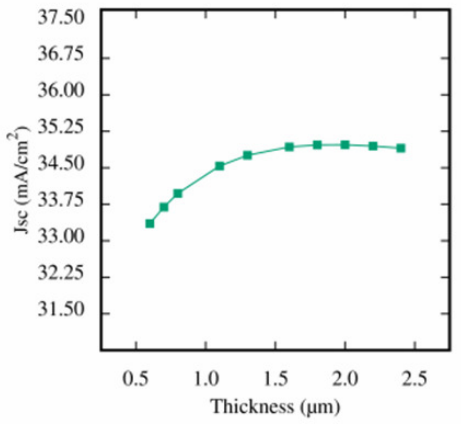

Fig. 4. Variation of solar cell short circuit current density versus the base layer thickness.

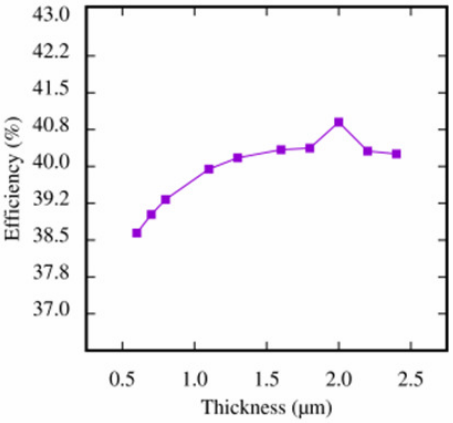

Fig. 5. Variation of solar cell efficiency versus the base layer thickness.

Fig. 2 shows that V_{OC} remains almost unchanged on the considered domain of thickness variation, except of a small increase at $2\mu m$ of thickness. Fig. 3 shows that the factor form is more affected by the thickness variation. This factor undergoes an increase from 89.2% to 90% when the thickness increases from $0.6\mu m$ to $2\mu m$. Then, it decreases before increasing slightly again. Fig. 4 shows that J_{sc} increases with increasing thickness of the base layer. A plateau is reached at $1.8\mu m$ of thickness where J_{sc} is not affected by the variation of thickness. Fig. 5 shows that efficiency of the GaAs/GaSb dual-junction solar cell is maximum with $\eta = 41\%$ at $2\mu m$ of thickness. Then, it decreases.

It is clear from this analysis that a base layer thickness of $2\mu m$ gives the highest efficiency.

3.1.2 Effect of doping concentration

Doping concentration is a key parameter to consider while designing a solar cell, because it directly affects the width of the depletion region. In the following, the effect of doping concentration on the cell electrical characteristics is analysed, when fixing the thickness of the base layer at its optimum value of $2\mu m$.

A parametric study was performed by varying the carriers concentration level from $2\times10^{15}\,cm^{-3}$ to $2\times10^{19}\,cm^{-3}$. Table 2 gives the obtained results in terms of the cell performance characteristics.

Table 2. Cell performance characteristics versus top GaAs base layer donor concentration.

$N_d\,(cm^{-3})$	$V_{OC}(V)$	$J_{sc}(mA/cm^2)$	$FF(\%)$	$\eta(\%)$
2×10^{15}	1.65	36.74	86.51	38.05
8×10^{15}	1.70	36.58	85.34	38.55
2×10^{16}	1.72	36.55	86.03	38.87
8×10^{16}	1.78	35.72	90.16	41.65
2×10^{17}	1.77	35.12	89.70	41.11
8×10^{17}	1.78	34.51	89.26	39.80
2×10^{18}	1.78	32.65	89.17	37.66
8×10^{18}	1.78	30.06	89.35	34.68
2×10^{19}	1.78	29.07	89.47	33.56

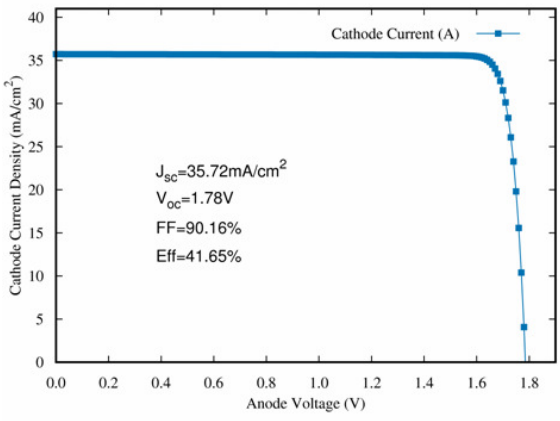

Fig. 6. I-V curve of the optimized InGaP/GaAs dual-junction solar cell as obtained in this work.

As shown from Table 2, J_{sc} value is affected by variation of donor doping in GaAs base layer. As the doping level increases, it decreases from the initial value of $36.74mA/cm^2$ to $29.07mA/cm^2$. This result is expected, because the doping concentration is inversely proportional to the depletion layer width. At moderate doping levels the width of this layer increases and leads to better performance. For the voltage V_{OC} values, it is seen that they show minor change at different carrier concentration. On the other hand, the form factor FF and the efficiency η increase until the doping level reaches $8\times10^{18}\,cm^{-3}$, then they decrease. Based on these observations, the ideal doping concentration can be fixed at $8\times10^{18}\,cm^{-3}$.

The obtained I-V curve of the improved GaAs/GaSb dual-junction solar cell is depicted in Fig. 6. The optimized structure reaches the maximum efficiency of 41.65 % with open circuit voltage $1.78V$, short circuit current density of $35.72mA/cm^2$ and a filling factor of 90.16 %.

3.2 Effect of sun light concentration on solar cell performance

The highly efficient multi-junction solar cells are habitually used in combination with Concentrator PhotoVoltaics (CPV). This technology uses cheap optical elements, like lenses, to concentrate light into small area of the expensive cell. This combination leads to highest efficiencies at economical cost. The light concentration ratio of 1 sun is the standard illumination AM1.5.

Considering the benefit of solar concentration, the impact of varying light intensity on the I-V characteristics of the optimized solar cell as found in this work is next studied. Table 3 and Fig. 7 give respectively the performance parameters and the I-V curves as function of the number of sun used in illumination.

Table 3. Solar cell parameters at different sunlight intensities.

Number of sun (X)	1	30	60	90	120
$J_{sc}(mA/cm^2)$	35.72	1073	2148	3235	4336
$V_{OC}(V)$	1.78	1.94	2	2.01	2.02
$FF(\%)$	90.16	90.65	88.5	82.9	73.03
$\eta(\%)$	41.85	45.73	45.78	41.65	38.72

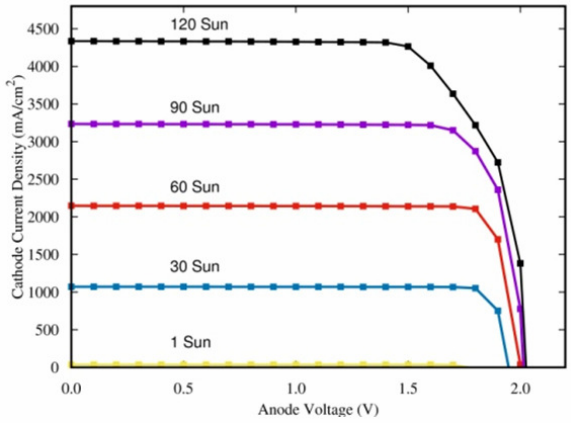

Fig. 7. I-V characteristics of the optimized InGaP/GaAs dual-junction solar cell as function of sunlight intensity.

From Table 3 and Fig.7, it can be seen that J_{sc} increases linearly with increased illumination level, while V_{OC} incremental increase is less pronounced. Table 3 shows that the power conversion efficiency attains its maximum value of 45.78% at 60sun. Then, the efficiency starts decreasing for higher concentration ratio. The sunlight concentration has a positive effect on solar cell performance but at specific ratio, otherwise the Joule effect will dominate and degrades efficiency.

The observed variations in terms of solar cell key parameters agree with established theoretical predictions when Joule effect is neglected. These are given by

$$J_{sc}(X) = J_{sc}(1) \times X \tag{5}$$

$$V_{OC}(X) = \frac{bk_B T_C}{q} \ln\left(\frac{J_{sc}(1) \times X}{J_0} + 1\right) \tag{6}$$

$$\eta = \eta_1 \frac{\ln\left(1 + J_{sc,\max}(1) \times X / J_0\right)}{\ln\left(1 + J_{sc,\max}(1) / J_0\right)} \tag{7}$$

where X is the number of sun and η_1 is that obtained for $X = 1$.

4 Conclusions

Optimisation of a GaAs/GaSb dual junction solar cell was performed numerically in this work. This was achieved trough investigating the impact of the GaAs base layer key parameters on the cell characteristics. These included its thickness and doping concentration level. It was found that the carrier concentration has a major effect on the main cell parameters, while the thickness does not affect largely the results. The simulations have enabled to fix the optimal configuration of the cell that provides the highest performance. This reached an efficiency of 41.65% with short current density of $35.72 mA/cm^2$ and open circuit voltage of $1.78V$. The effect of sunlight concentration was also investigated. The optimum concentration ratio was found to be 60sun. This gives an efficiency of 45.78%. Above 60sun, the efficiency decreases due to the power losses caused by electric resistance.

References

1. M. S. Leite, R. L. Woo, J. N. Munday, W. D. Hong, S. Mesropian, D. C. Law, H. A. Atwater, Appl. Phys. Lett. **102**, 033901 (2013)
2. K. Tanabe, Energies **2** (2009)
3. M.A. Green, K. Emery, Y. Hishikawa, W. Warta, E.D. Dunlop, Prog. Photovolt. **21**, 5 (2013)
4. J. Nikoletatos, G. Halambalakis, *Standards, Calibration, and Testing of PV Modules and Solar Cells*, (McEvoy's Handbook of Photovoltaics, Academic Press, 2018)
5. C. Cornet, M. Da Silva, C. Levallois, O. Durand, *GaP/Si-Based Photovoltaic Devices Grown by Molecular Beam Epitaxy* (MBE, From Research to Mass Production, Second Edition, Elsevier, 2018)
6. Y. Guo, Q. Liang, B. Shu, J. Wang, Q. Yang, Int. J. Photoenergy **10** (2018)
7. R. Oshima, Y. Nagato, Y. Okano, T. Sugaya, Jap. J. Appl. Phys. **57** (2018)
8. G.S. Sahoo, G.P. Mishra, Superlattices Microstruct. **109** (2017)
9. L. Fraas, B. Daniels, H.X Huang, J. Avery, C. Chu, P. Iles, P. Piszczor, *Over 30% efficient InGaP/GaAs/GaSb cell-interconnected-circuits for line-focus concentrator arrays* (Proc. of the 28th Photovoltaic Specialists Conference, IEEE, 2000)
10. J.A. Hutchby, R.J. Markunas, S.M. Bedair, *Material Aspects Of The Fabrication Of Multijunction Solar Cells* (Proc. SPIE 0543, Photovoltaics, 1985)
11. J. Simon, D.M. Roberts, J. Boyer, K.L. Schulte, A. Braun, A.N. Perna, A.J. Ptak, *Recent HVPE grown solar cells at NREL* (Proc. of the 48th Photovoltaic Specialists Conference (PVSC), IEEE, 2021)
12. K.L. Schulte, J. Simon, A.J. Ptak, Prog. Photovoltaics **26**, 11 (2018)
13. Y. Shoji, R. Oshima, K. Makita, A. Ubukata, T. Sugaya, Solar RRL **6**, 4 (2021)
14. S.S. Soley, A.D.D. Dwivedi, Mater. Today: Proc., **39** (2021)
15. L.M Frass, J.E Avery, V.S. Sundaram, V.T. Kinh, T.M. Davenport, J.W. Yerkes , J.M. Gee, K.A. Emery, *Over 35% efficient GaAs/GaSb stacked concentrator cell assemblies for terrestrial applications* (Proc. of the 21st IEEE Photovoltaic specialists conference, IEEE, 1990)
16. L. Fraas, J. Avery, R. Ballantyne, W. Daniels, III-Vs Review **12** (1999)
17. R. Szweda, III-Vs Rev. **14**, 8 (2001)
18. J.M. Olson, D.J. Friedman, S. Kurtz, *High-Efficiency III–V Multijunction Solar Cells* (In Handbook of Photovoltaic Science and Engineering, 1st ed, Wiley, 2003)
19. G.S. Sahoo, G.P. Mishra, J. Electron. Mater. **48** (2019)
20. F.Z. Kharchich, A. Khamlichi, Optik **272** (2023)
21. K.J. Singh, S.K. Sarkar, Opt. Quant. Electron. **43** (2012)
22. A.D.D. Dwivedi, P. Chakrabarti, Int. J. Adv. Appl. Phys. Res. **2**, 1 (2015)
23. Silvaco International, *ATLAS User's Manual* (Silvaco International, Santa Clara, 2019)
24. A.O.M. Maka, T.S. O'Donovan. Therm. Sci. Eng. Progress **10** (2019)
25. E.T. Mohamed, A.O.M. Maka, M. Mehmood, A.M. Direedar, N. Amin, Sustain. Energy Technol. Assess. **44** (2021)